tvst

Retina

Homozygous Knockout of *Cep250* Leads to a Relatively Late-Onset Retinal Degeneration and Sensorineural Hearing Loss in Mice

Alaa Abu-Diab[1,*], Prakadeeswari Gopalakrishnan[1,*], Chen Matsevich[1], Marije de Jong[2], Alexey Obolensky[1], Ayat Khalaileh[1], Manar Salameh[1], Ayala Ejzenberg[1], Menachem Gross[2], Eyal Banin[1], Dror Sharon[1,], and Samer Khateb[1,**]**

[1] Department of Ophthalmology, Hadassah Medical Center, Faculty of Medicine, The Hebrew University of Jerusalem, Jerusalem, Israel
[2] Department of Otolaryngology, Head and Neck Surgery, Hadassah Hebrew-University Medical Center, Jerusalem, Israel

Correspondence: Samer Khateb, Department of Ophthalmology, Hadassah Medical Center, Faculty of Medicine, The Hebrew University of Jerusalem, Ein kerem, Jerusalem 91120, Israel.
e-mail: samerkhateb@gmail.com

Received: February 16, 2022
Accepted: January 24, 2023
Published: March 1, 2023

Keywords: *CEP250*; knockout; hearing loss; retinal degeneration; Usher syndrome

Citation: Abu-Diab A, Gopalakrishnan P, Matsevich C, de Jong M, Obolensky A, Khalaileh A, Salameh M, Ejzenberg A, Gross M, Banin E, Sharon D, Khateb S. Homozygous knockout of *Cep250* leads to a relatively late-onset retinal degeneration and sensorineural hearing loss in mice. Transl Vis Sci Technol. 2023;12(3):3, https://doi.org/10.1167/tvst.12.3.3

Purpose: Usher syndrome (USH) is the most common syndromic inherited retinal disease, causing retinitis pigmentosa and sensorineural hearing loss. We reported previously that a nonsense mutation in the centrosome-associated protein *CEP250* gene (encoding C-Nap1) causes atypical USH in patients of Iranian Jewish origin. To better characterize *CEP250*, we aimed to generate and study a knockout (KO) mouse model for *Cep250*.

Methods: Mice heterozygous for a "knockout-first" *Cep250* construct were generated and bred with Cre recombinase mice to generate the null allele and produce homozygous *Cep250* KO mice. Retinal function was evaluated by full-field electroretinography (ffERG) at variable ages, and retinal structure changes were examined using histological analysis. Hearing thresholds were detected using auditory brainstem response (ABR) at the age of 20 months.

Results: The *Cep250* KO mouse model was generated by activating a construct harboring a deletion of exons 6 and 7. At 6 months, the ffERG was normal, but it decreased gradually with age. For both photopic and scotopic ffERG responses, very low amplitudes were evident at 20 months. Histological analysis confirmed late-onset retinal degeneration. ABR tests illustrated that hearing threshold significantly increased at the age of 20 months.

Conclusions: Although most USH animal models have normal retinal function and structure, the *Cep250* KO mouse model shows both retinal degeneration and hearing loss with a relatively late age of onset. This model may shed more light on *CEP250*-associated retinal and hearing deficits and represents an efficient platform for the development of treatment modalities for USH.

Translational Relevance: Our study demonstrates better understanding of *Cep250*-associated retinal and hearing disease in a mouse model and may help in developing more efficient gene therapy modalities.

Introduction

Inherited retinal diseases are genetically and phenotypically heterogeneous groups of eye disorders caused by inherited genetic mutations. More than 300 genes and loci are associated with inherited retinal diseases (refer to RetNet at https://sph.uth.edu/retnet/). Retinitis pigmentosa (RP) is the most common inherited retinal disease, with a prevalence of 1 out of 4000 people around the world[1] and a higher prevalence in the vicinity of Jerusalem.[2] Patients with RP typically lose their night vision at a young age, peripheral vision in adulthood, and central vision at an older

age as a result of progressive loss of photoreceptor cells in the retina. Most patients with RP (70%–80%) suffer from vision loss alone without any other clinical deficit, referred as non-syndromic RP. When RP occurs in association with a systemic disease, involving other tissues in the body, it is termed syndromic RP. Usher syndrome (USH) is the most common type of syndromic RP,[3] in which patients suffer from RP, sensorineural hearing loss (SNHL), and vestibular areflexia in some cases. This syndrome is heterogeneous, in both clinical and genetic aspects, and can be classified into three major subtypes according to the varied clinical symptoms observed in patients, specifically the severity and progression of hearing loss and onset age of RP. USH type I is characterized by congenital SNHL associated with vestibular areflexia, followed by early-onset RP in the first decade of life. USH type II is characterized by mild to moderate non-progressive SNHL and typical RP, which starts within the second decade without balance problems. In USH type III, hearing impairment develops at childhood or in the early teens, with a variable age of onset of RP. In USH type III, relatively late onset (around the age of 40 years) of RP and SNHL without vestibular involvement has been reported.[4] All types of USH syndrome are inherited in an autosomal recessive manner.[5] Lately, there have been numerous reports of USH cases that do not fit any of the classical types of the syndrome, and these are termed atypical USH.[6–8]

In a previous study,[7] we reported that a novel homozygous nonsense mutation in *CEP250,* encoding the centrosome-associated protein CEP250 (also known as C-Nap1), causes atypical USH in patients from a relatively large, single family of Iranian Jewish descent. In addition to the *CEP250* mutation, patients were either homozygous or heterozygous for a nonsense mutation in *C2orf71*. The double homozygous patients suffered from early-onset severe RP and early-onset severe SNHL, whereas patients who were homozygous for the *CEP250* mutation and heterozygous for the *C2orf71* mutation had a milder retinal phenotype.[7] CEP250 belongs to the CEP family of proteins that includes over 30 members that compose the active component of the centrosome and are required for centriole–centriole cohesion during interphase of the cell cycle. C-Nap1 was previously reported to be expressed in photoreceptor cilia and is known to interact with other ciliary proteins, including Rootletin and NEK2.[9,10] Following our original report, additional families were reported with biallelic *CEP250* mutations: a homozygous missense variant (p.A609V) in patients with atypical RP,[11] compound heterozygous nonsense mutations (c.361C>T, p.R121* and c.562C>T, p.R188*) in two Japanese patients with mild cone–rod dystrophy (CRD) and SNHL,[12] compound heterozygous nonsense mutations (p.K1113* and p.R1336*) in a case with progressive hearing loss and late-onset CRD,[13] a homozygous nonsense mutation (c.562C>T) in a patient with RP (the patient was followed until the age of 28 years),[14] and three USH cases with biallelic truncated mutations.[15]

Multiple mouse mutants of retinal diseases are already recognized or can be generated relatively easily for investigations. Studies with USH mouse models helped us obtain most of our knowledge regarding the function of USH proteins, including the defective myosin VII a (shaker-1),[16] and some of the spontaneous mouse mutants, including *Pcdh15* (Ames waltzer), Whirlin (whirler), and the Ush2A$^{-/-}$ mouse model.[17–19] Despite that, most of these USH mouse models show severe hearing loss and vestibular dysfunction, but none except the Ush2A$^{-/-}$ mouse has shown any signs of the RP that is observed in USH patients.[20] A knock-in (KI) mouse model for *Cep250*–p.R176* (corresponding to the human mutation p.R188*) was shown to have RP; however, no hearing evaluation was performed.[14] In the current study we created and characterized visual and hearing properties of a knockout (KO) mouse model for *CEP250* showing a relatively mild and late-onset USH phenotype, similar to the human presentation.

Methods

Generation of the *Cep250* KO Mouse Allele

Heterozygous mice for a "knockout-first" allele (tm1a)[21] within the *Cep250* gene (C57BL/6NA^{tm1Brd} *Cep250*$^{tm1a(EUCOMM)Wtsi/Wtsi}$) were purchased from the Sanger Institute Mouse Genetics Programme (Sanger MGP, Cambridgeshire, UK). The construct was inserted instead of a genomic region that includes exons 6 and 7 of *Cep250*. Mice were maintained in a specific-pathogen-free unit, housed in filter-top cages in an air-conditioned environment on a 12-hour light/dark cycle at 22°C, and had free access to water and food. All procedures were approved by the Animal Ethics Committee of the Hebrew University–Hadassah Medical School and adhere to the ARVO Statement for the Use of Animals in Ophthalmic and Vision Research.

Breeding and Construct Activation

We used the Cre/LoxP strategy to activate the construct and generate homozygous *Cep250* KO

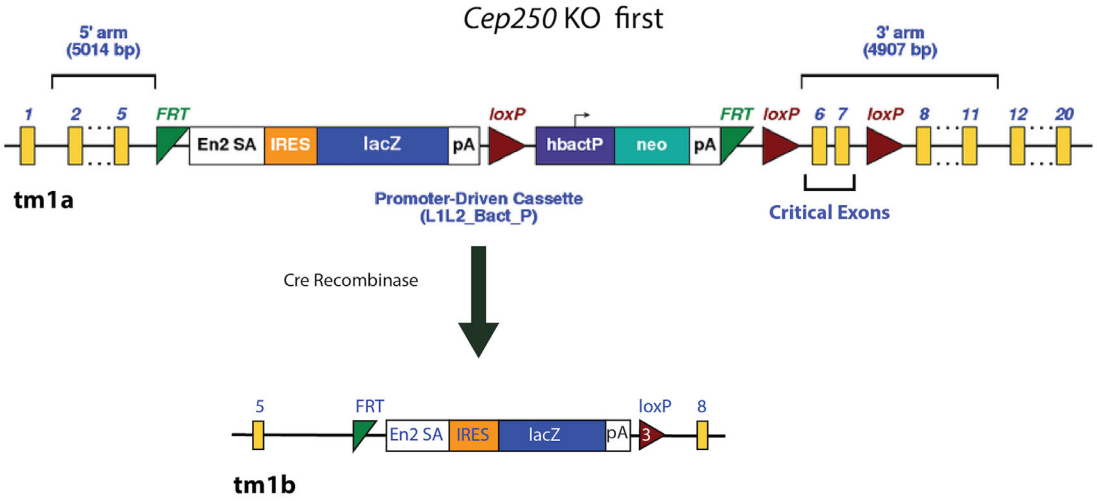

Figure 1. Gene targeting strategy to KO exons 6 and 7 of *Cep250*. In the targeting construct, first KO allele (tm1a), the critical exons (6 and 7) were flanked by loxP sites. Mice carrying the mutant floxed allele were crossed with transgenic C57Bl/6 mice carrying Cre recombinase. Cre deletes the promoter-driven selection cassette and floxed exon of the (tm1a) allele to generate a *lacZ*-tagged allele (tm1b). *Yellow blocks* indicate the homolog exons of *Cep250* on both sides of the construct.

mice. Heterozygous male mice with a non-activated construct were bred with homozygous Cre recombinase female mice to produce $Cep250^{-/wt}CRE^{+/-}$ offspring in which the construct is activated, causing deletion of exons 6 and 7 (Fig. 1). These offspring were bred to generate the homozygous $Cep250^{-/-}$ KO mice.

DNA Extraction From Mouse Tissue

Genomic DNA was extracted from ear punch or tail samples by using the KAPA Express Extract Kit (KR0383; Kapa Biosystems, Wilmington, MA), or by adding 180 µL of 50-mM NaOH to 5 to 10 mg of mouse tissue, followed by incubation for 10 minutes at 95°C and neutralizing the extract after that with 20 µL of 1-M Tris HCl (pH 8.0).

PCR Primers and Conditions

Polymerase chain reaction (PCR) was used to identify the *Cep250* KO allele using primers listed in Table 1 and the KAPA Mouse Genotyping Kit (KR0385; Kapa Biosystems) or the 2x PCRBIO HS Taq Mix Red Kit (PB10.23.02; PCR Biosystems, London, UK).Thermal cycling conditions were primary denaturation at 94°C for 10 minutes; 40 cycles of denaturation at 94°C for 30 seconds, annealing at 60°C for 30 seconds, and DNA extension at 72°C for 30 seconds; and a final extension cycle at 72°C for 5 minutes.

RNA Extraction and Reverse-Transcription PCR

Total RNA was extracted from mice retinas using TRI Reagent (T9424; Sigma-Aldrich, St. Louis, MO).

Table 1. Primers Used for Mice Genotyping

Primer Name	Amplification	Primer Sequence
cep250-F	Exon5-Inron5	GCAGGAGGACGTGGAAAAAC
cep250-R	Exon5-Inron5	GAACCCAGCAAAGGTTCAGG
CAS-R1-TermR	Exon5- construct	TCGTGGTATCGTTATGCGCC
cep250 5arm-F	Inrton5	AGTTCTCTTCCTAGTTCTGCCT
cep250-crit-WTR	Inrton5	TGGGTGGCCTAATACATGCA
5mut-R1	Intron5 -1st FRT	GAACTTCGGAATAGGAACTTCGGTT
crit-WTF	Intron5-Intron7	GAAGGCCACTTTTCATCCAG
3arm-WTR	Intron5-Intron7	GCCACCCCAAAGAGGACA
lacZ-PF	lacZ-intron5	CCAGTTGGTCTGGTGTCA
crit-R	Intron5-Exon7	TCTTAGCGACGAGCAGCAG

Table 2. Primers Sequence and Amplification for RT-PCR

Primer Name	Primer Amplification	Primer Sequence
CEP250-M-Ex5-6F	ex5-6	GCGAGAGGTGGTAACCTTCC
CEP250-M-Ex5-6R		TTCTCATGGGCTTCCTTCTC
CEP250-M-Ex1-2F	ex1-2	GTTGAACATGAAGCCCCAGT
CEP250-M-Ex1-2R		GGCTTCTAGTCGCTTCTCCA
CEP250-M-Ex3-4F	ex3-4	AGCGCTGGGAGAGTGTAGAA
CEP250-M-Ex3-4R		CCACTGGCTCTCCTTCCTC
CEP250-M-Ex7-9F	ex7-9	TGCTAACCCAGTCTCAGAAGC
CEP250-M-Ex7-9R		GGGTCCTGGGGATCAAAC
CEP250-M-Ex26-27F	ex26-27	GGAAGGGAGGCAGAACTCC
CEP250-M-Ex26-27R		GACCTCCCGCTCTCTGTTAG

Reverse-transcription PCR (RT-PCR) was performed using the Verso cDNA Synthesis Kit (AB-1453/B; Thermo Fisher Scientific, Waltham, MA) and C1000 Thermal Cycler (Bio-Rad, Hercules, CA) following the manufacturer's protocol. Primers were designed using Primer3 software (http://bioinfo.ut.ee/primer3-0.4.0/) (Table 2).

Full-Field Electroretinography

Full-field electroretinography (ffERG) was performed on anesthetized animals following overnight dark adaptation using a Ganzfeld dome and a computerized system (Espion E2; Diagnosys LLC, Lowell, MA). Mice were anesthetized by intraperitoneal injections of a mixture of ketamine (Bedford Laboratories, Bedford, OH) and xylazine (VMD, Arendonk, Belgium), using body weight–adjusted doses. Pupils were dilated with 1% tropicamide and 2.5% phenylephrine, and local anesthetic drops (benoxinate HCl, 0.4%; all ocular drops from Fisher Pharmaceuticals, Tel-Aviv, Israel) were administered prior to placing gold-wire active electrodes on the central cornea. A reference electrode was placed on the tongue and a needle ground electrode was placed intramuscularly in the hip area. Dark-adapted rod and mixed cone–rod, as well as light-adapted 1-Hz and 16-Hz cone flicker responses to a series of white flashes of increasing intensities (0.00008–9.6 cd·s/m^2) were recorded. All ffERG responses were filtered at 0.3 to 500 Hz, and signal averaging was applied.

Auditory Brainstem Response Test

Auditory brainstem response (ABR) was measured in *Cep250*$^{-/-}$ mice and controls using evoked potential recording in anesthetized mice. Mice were anesthetized intraperitoneally prior to ABR recordings. The ABR was recorded for air conduction in each mouse in response to alternating polarity broadband clicks presented by an insert earphone in the external ear canal (Navigator Pro System; Biological Systems Corporation, Mundelein, IL). Recording subdermal needle electrodes were inserted in the skin at the vertex between the ears with reference to the chin and a ground electrode in the right hind limb. Stimuli were presented at a rate of 20 per second from a maximal intensity of 120-dB sound pressure level down to threshold in 5-dB steps. The recorded activity was bandpass filtered (300–3000 Hz) and averaged (n = 128 to 256 responses). Threshold was defined as the lowest stimulus intensity with a clear repeatable component (usually the first wave) in at least two out of three ABR recordings.

Paraffin Embedding

Adult mice were killed with an overdose of the anesthetic mix or using the carbon dioxide chamber. Their eyes were fixed in Davidson solution, dehydrated, and embedded in paraffin. The eyes were sectioned using a RM2145 microtome (Leica, Wetzlar, Germany) into 5-µm-thick sections through the center of the optic nerve, moved to the surface of a 37°C water bath, floated to positive-charged slides for immunohistochemistry (Superfrost Plus, 4951PLUS4; Thermo Fisher Scientific) or to precleaned slides (color-frosted, BN1045001C; Bar-Naor Ltd., Petah Tikva, Israel), and kept at 37°C overnight.

Histological and Immunostaining Analyses

Sections for histological analysis were deparaffinized in Clear Care Plus solution (xylene substitute 1276; Kaltek, Padua, Italy), rehydrated, and stained in hematoxylin and eosin (H&E) solution. All observations and photography were performed using an

Olympus BX41 microscope equipped with a DP70 digital camera (Olympus, Tokyo, Japan). Sections for immunohistochemistry were deparaffinized in xylene, dehydrated in graded alcohols, and rinsed with phosphate-buffered saline (PBS, pH 7.4, P3813; Sigma-Aldrich). For antigen retrieval, they were incubated in a decloaking chamber with 10-mM sodium citrate buffer with 0.05% Tween 20 (pH 6.0) at 125°C for 10 minutes. The slides were then cooled down to room temperature and blocked for 1 hour with 10% normal donkey serum in PBS solution (pH 7.4, P3813; Sigma-Aldrich) and 0.1% Triton X-100 at room temperature. Subsequently, sections were incubated overnight at 4°C in a humid chamber with the polyclonal antibody C-Nap1 (E-19) 1:100 (sc74349; Santa Cruz Biotechnology, Dallas, TX). After they were washed with PBS, the slides were incubated with DyLight 488 Donkey anti-Rabbit (1:250; Jackson Immuno Research Laboratories, West Grove, PA). Sections were washed in double distilled water, and nuclei were counterstained with 4′,6-diamidino-2-phenylindole (71-03-01; SeraCare, Mildord, MA). The slides then were mounted with VECTASHIELD mounting medium (H1000; Vector Laboratories, Newark, CA). An Olympus BX41 microscope equipped with a DP70 digital camera was used for observations and photography.

Results

Because a large number of centrosomal proteins were reported to cause inherited retinal diseases when mutated, we aimed to generate a KO mouse model for *CEP250* and study the phenotype of mice lacking expression of this gene. Heterozygous mice (C57BL/6N-Atm1Brd *Cep250*$^{tm1a(EUCOMM)Wtsi/H}$) for the "knockout-first" allele (tm1a) were generated by an outsourced company. By breeding them with Cre recombinase homozygous mice, the "knockout-first" allele (tm1a) was converted to the null (tm1b) allele,[21] producing homozygous *Cep250* KO mice harboring the deletion of exons 6 and 7. This exon deletion produces a frameshift mutation (c.597_945del, p.Asp200Argfs*7) that might be translated to form a truncated protein that is nonfunctional or degraded by the nonsense-mediated mRNA decay pathway.

Shorter RNA is Expressed in the Retina of Homozygous *Cep250* KO Mice

In order to study the effect of exon 6 and 7 deletion on *Cep250* expression, RNA was extracted from KO and wild-type (WT) mouse retina. RT-PCR was done using primers located along the cDNA transcript (Fig. 2, Table 2). In the retina of *Cep250*$^{-/-}$ mice, only exons 1 to 5 could be amplified, and no RT-PCR product was obtained for the remaining exons, compared to a normal expression pattern in WT mice (Fig. 2).

Full-Field ERG Recording in WT and KO Mice

The ffERG was performed on anesthetized animals following overnight dark adaptation to evaluate retinal function. No significant difference between KO and WT mice was obtained in either scotopic (Figs. 3A, 3B) or photopic (Figs. 3C, 3D) ERG conditions at the age of 6 months. Testing at ages 12 and 20 months showed 42% and 71% decrease in the a- and b-wave amplitudes of KO compared to WT mice, respectively. Representative scotopic ERG responses at the age of 20 months are shown in Supplementary Figure S1. Light-adapted ffERG of KO mice at 12 months showed only an 11% decrease in responses compared to the WT controls, whereas at 20 months of age a significant decline of 82% was evident.

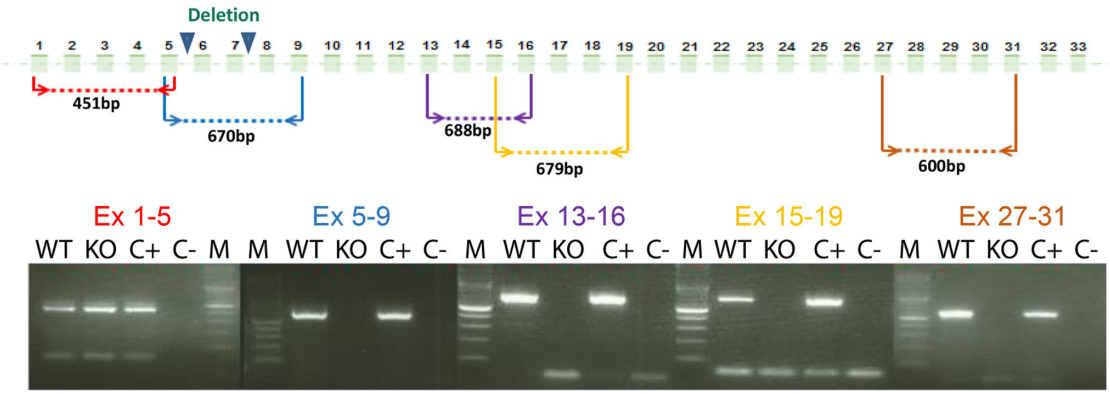

Figure 2. RT-PCR analysis of *Cep250* mRNAs in the mouse retina. RNA was extracted from mouse retina at the age of 6 months. C+, positive control that does not contain the *Cep250* construct; C–, negative control without cDNA; M, DNA marker.

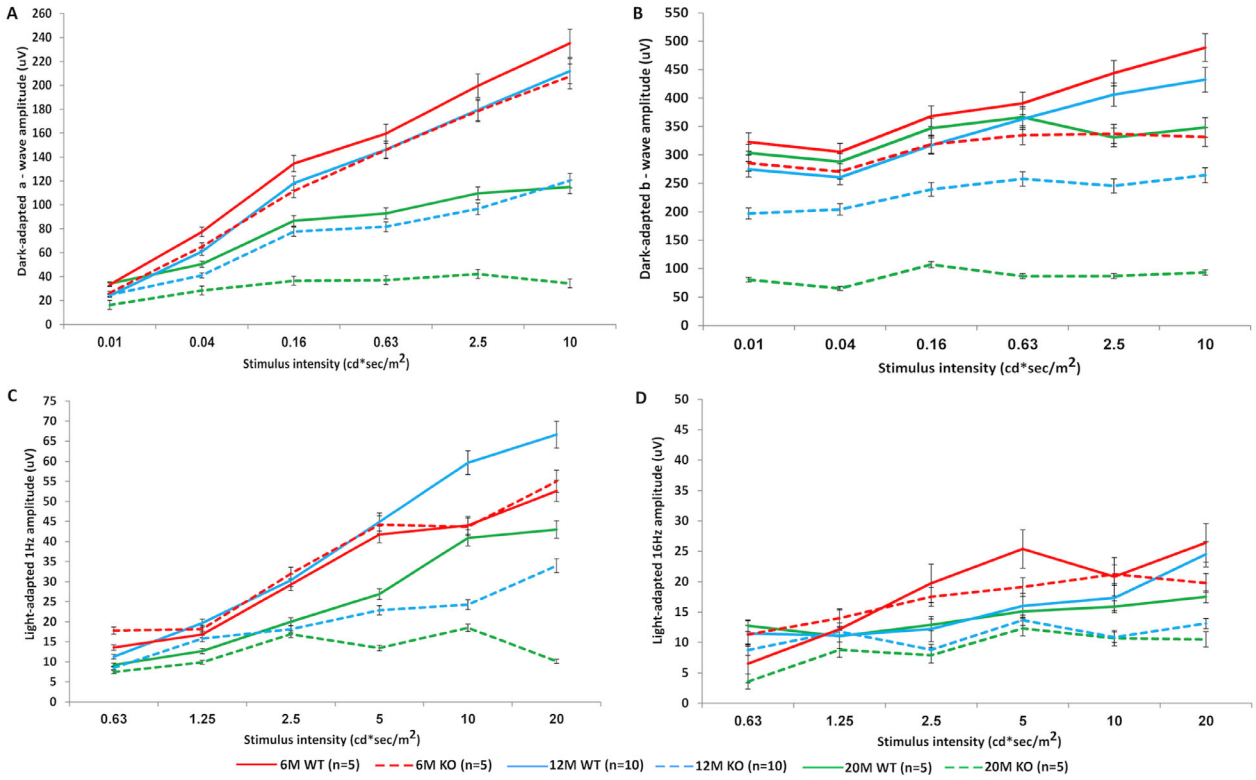

Figure 3. Results of ffERG. Amplitudes of dark-adapted (A, B) and light-adapted (C, D) ffERG responses in 6-, 12-, and 20-month-old (M) *Cep250* KO mice revealed progressive deterioration of retinal function over time. The scotopic a-wave responses at higher intensities for 20M KO mice showed a trend toward lower amplitudes (A), and b-wave amplitudes were markedly reduced compared to WT mice and 6M KO mice (B). Light-adapted 1-Hz and 16-Hz flicker responses were also markedly reduced in KO mice at 12 and 20 months (C, D).

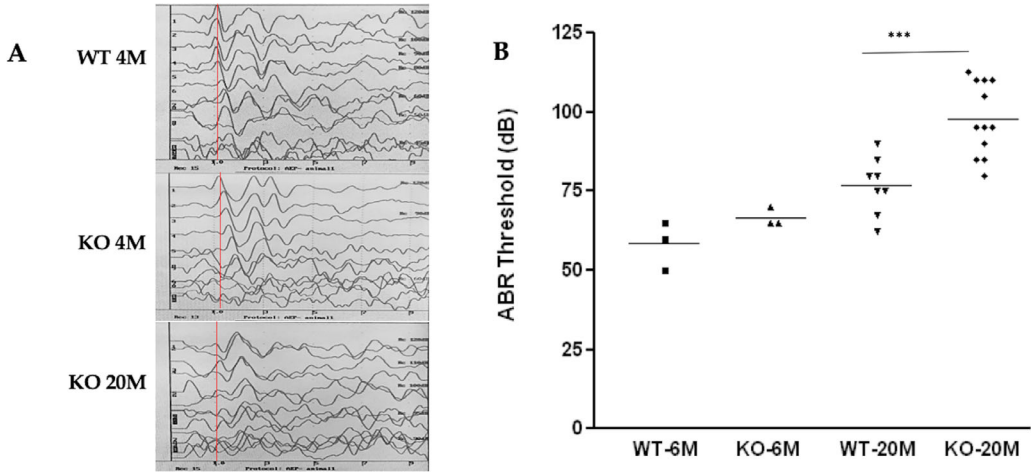

Figure 4. Auditory brainstem responses. (A) Representative ABR tracings from WT and *Cep250* KO mice. WT mice presented normal ABR waveforms, but the deaf mice presented no identifiable ABR responses. The *red line* marks the first wave out of five for 4M WT mice, 4M KO mice, and 20M KO mice. The *x*-axis is time (msec), the *y*-axis is intensity (dB). (B) Summary of all ABR data.

Auditory Brainstem Response

To complete the phenotype analysis of the *Cep250* KO mouse model, mice were tested for ABR following the ffERG tests. ABR thresholds were tested at 4 and 20 months of age, illustrating that the hearing threshold significantly increased for the KO mice at the age of 20 months (Fig. 4). Representative ABR tracings for WT mice and KO at different ages (Fig. 4A) show that ABR waves became less clear in the KO mice with age. But, it

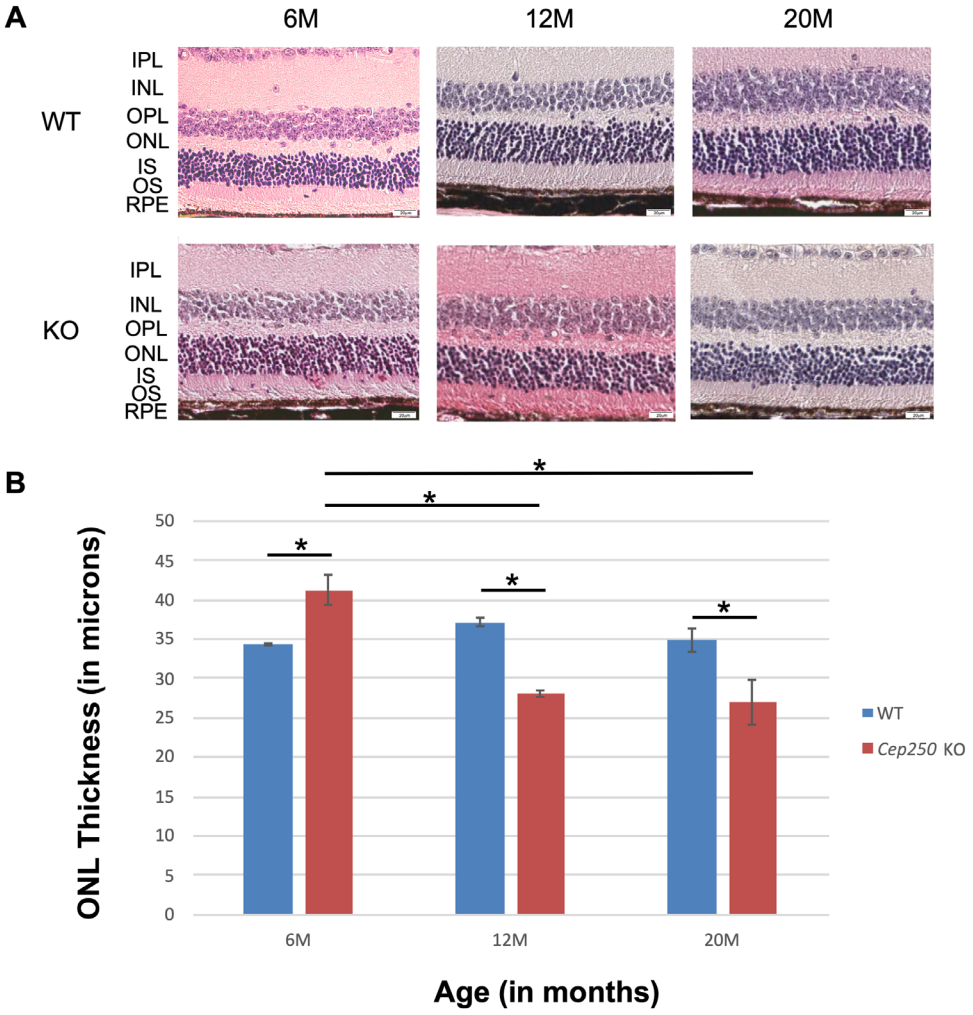

Figure 5. Retinal histology in *Cep250* KO and WT mice. (A) Representative images of mid-peripheral retina stained with H&E. Original magnification, 20×. M, month; IPL, inner plexiform layer; INL, inner nuclear layer; OPL, outer plexiform layer; ONL, outer nuclear layer; IS, inner segment; OS, outer segment; RPE, retinal pigment epithelium. (B) Bar graph of ONL thickness in WT (6M, $n = 12$; 12M, $n = 16$; 20M, $n = 8$) versus *Cep250* KO (6M, $n = 8$; 12M, $n = 4$; 20M, $n = 6$) in the midperipheral retina. Statistically significant differences ($P < 0.001$) based on Student's *t*-test analysis are indicated with an asterisk above a line connecting the two appropriate groups.

was interesting to see that the hearing deterioration in the KO mice was significantly worse compared to their age-matched WT mice, whereas in the younger ages this difference between WT and KO mice was less profound (Fig. 4B).

Histological and Immunostaining Analyses of Cep250$^{-/-}$ Retina

Mice were sacrificed following the ABR test, their eyes were enucleated, and histological analysis was performed using H&E staining at different ages for both WT and KO *Cep250* mice (6, 12, and 20 months of age). Although the WT mice did not show significant differences in outer nuclear layer (ONL) thickness between the different time points, KO mice at the age of 12 and 20 months showed ONL thinning compared to KO at 6 months and to age-matched WT retina (Figs. 5A, 5B; Supplementary Fig. S3). Immunostaining analysis was performed with the Cep250 and Cep78 antibodies on Cep250$^{-/-}$ retina at the age of 6 months. In the WT retina, both antibodies labeled the junction between photoreceptor inner and outer segments, indicating, as expected, ciliary localization (Supplementary Figs. S2A and S2C, marked with white arrows). On the other hand, diffused Cep78 staining is evident in the Cep250$^{-/-}$ retina (Supplementary Fig. S2B), indicating disorganized cilia, and no Cep250 expression is evident in the Cep250$^{-/-}$ retina (Supplementary Fig. S2D).

Discussion

In this project we generated a *Cep250* KO mouse model and characterized its phenotype as a model for Usher syndrome. We verified the mutation at the DNA level and showed that the mutant allele produces a shortened and mutated mRNA molecule lacking most coding exons starting from exon 6, indicating that the nonsense mRNA decay surveillance mechanism does not degrade aberrant *Cep250* RNA molecules in the mouse retina. In addition, ffERG and ABR evaluations revealed that the KO mice have decreased b-wave responses compared to the WT mice in dark-adapted conditions, decreased cone function at relatively older ages (similar to the phenotype observed in human *CEP250* patients suffering from late-onset RP), and a severe decrease in the hearing function in the KO mice compared to the age-matched WT. Both ffERG and ABR findings indicate a functional role of C-Nap1 in the retina, specifically in the ONL, and in the inner ear, augmenting our previous results associating *CEP250* mutations with atypical Usher syndrome.[7] As we reported previously, these patients harbored not only the homozygous *CEP250* mutation but also additional mutation in *C2orf71*, which is known to cause autosomal recessive RP.[22] Patients who are homozygous for the two mutations in both genes suffer from early-onset severe RP, in contrast to patients who are homozygous only for the *CEP250* mutation (and heterozygous for the *C2orf71* mutation), who have relatively mild RP. We are suggesting that the presence of the two mutations together worsen the RP expression in a patient's retina; therefore, it might be interesting to examine the effect of double KO mice for *Cep250* and *C2orf71*, as the phenotype of our *Cep250* KO mouse model mimics the phenotype of the patient with only the *CEP250* mutation.

To date, a few additional families were reported with biallelic *CEP250* mutations. In general, biallelic *CEP250* cases have RP with a variable age of onset from childhood to adulthood, and most (and possibly all) cases have late-onset hearing loss.[11–15] Cases in which hearing loss was not reported were either too young to present hearing loss or were not tested for this phenotype. In three cases,[15,23] a cone>rod phenotype has been reported, expanding the clinical spectrum of *CEP250* mutations. This variability is likely to be the result of modifier genes.

Recently, a *Cep250* KI mouse model for p.R176* (corresponding to the human mutation p.R188*) has been generated and followed up until the age of 1 year. Huang et al.[14] reported normal ERG and retinal histology at the age of 3 months and some reduction at the age of 6 months. This is considered a relatively slow retinal degeneration process in mouse models. In addition, the ERG light intensities used were higher compared to the current study; therefore, they showed a larger difference between the WT and KI models. When the same light intensities are compared, the differences between the KI and KO models are relatively small, with the KI model showing a slightly more severe disease progression. This can be due to mutations in other genes that cause retinal degeneration as reported in other strains[24,25] and were not studied in the KI model.[14] Such mutations were ruled out in our KO model. Alternatively, a mutant protein is being produced in the KI retina that might be toxic, leading to a more severe phenotype. This is supported by the intense labeling of the KI retina at the age of P45.[14] The authors reported significantly reduced retinal thickness and ERG responses, first noticed at the age of 3 months, indicating a late-onset RP phenotype.[14] Because no hearing evaluation was performed for this mouse model, it is unknown whether these mice had abnormal hearing, as identified in the KO mouse model we are presenting in the current study.

The mouse model we describe here can be further studied for better understanding of proteins that are involved in Usher syndrome. Some of the known mouse models for Usher syndrome were identified due to their characteristic circling and head-tossing behavior indicating vestibular dysfunction, but no retinal abnormalities were evident in these mouse models.[26] To the best of our knowledge, the *Cep250*$^{-/-}$ mice we present here are one of a few animal models that have been published as models for Usher syndrome and show both retinal degradation and hearing loss, although at a relatively late onset. Similarly, A/J *Clrn1*$^{-/-}$ mice were reported as a model for USH type 3, showing defect in the scotopic ERG responses only and no differences in photopic ERG responses between *Clrn1*$^{-/-}$ and WT mice, suggesting that the defect initiates from rod photoreceptors with delayed onset of hearing loss.[27,28] Recently, another group established a spontaneous mutant USH mouse model by crossing two strains together (hearing-impaired KM$^{ush/ush}$ mice with CBA/CaJ mice), thus the two phenotypes were caused by two different mutations.[29] In addition, two zebrafish models for Usher syndrome were recently reported.[30,31] Except for the *Ush2A*$^{-/-}$ mouse model,[19] the USH syndrome phenotype in all of the other mouse models that have been published is a result of two different mutations in two genes. The mouse model we describe here shows late-onset RP and progressive hearing loss as the result of KO in the *Cep250* gene only. Further studies using this model may help our understanding of the mechanisms of hearing loss and

retinal degeneration in patients with Usher syndrome, improving the speed and ease of developing therapies to prevent the retinal degeneration.

Acknowledgments

Supported by grants from the Israel Science Foundation (2154/15 to SK) and the Chief Scientist Office of the Israeli Ministry of Health and the Lirot Association (300009177 to SK).

Disclosure: **A. Abu-Diab**, None; **P. Gopalakrishnan**, None; **C. Matsevich**, None; **M. de Jong**, None; **A. Obolensky**, None; **A. Khalaileh**, None; **M. Salameh**, None; **A. Ejzenberg**, None; **M. Gross**, None; **E. Banin**, None; **D. Sharon**, None; **S. Khateb**, None

[*] AAD and PG contributed equally as first authors.
[**] DS and SK contributed equally as senior authors.

References

1. Hamel C. Retinitis pigmentosa. *Orphanet J Rare Dis*. 2006;1:40.
2. Sharon D, Banin E. Nonsyndromic retinitis pigmentosa is highly prevalent in the Jerusalem region with a high frequency of founder mutations. *Mol Vis*. 2015;21:783–792.
3. Tsang SH, Aycinena ARP, Sharma T. Ciliopathy: Usher syndrome. In: *Advances in Experimental Medicine and Biology*, Vol. 1085. New York: Springer; 2018:167–170.
4. Khateb S, Kowalewski B, Bedoni N, et al. A homozygous founder missense variant in arylsulfatase G abolishes its enzymatic activity causing atypical Usher syndrome in humans. *Genet Med*. 2018;20(9):1004–1012.
5. Mathur P, Yang J. Usher syndrome: hearing loss, retinal degeneration and associated abnormalities. *Biochim Biophys Acta*. 2015;1852(3):406–420.
6. Bashir R, Fatima A, Naz S. A frameshift mutation in SANS results in atypical Usher syndrome. *Clin Genet*. 2010;78(6):601–603.
7. Khateb S, Zelinger L, Mizrahi-Meissonnier L, et al. A homozygous nonsense CEP250 mutation combined with a heterozygous nonsense C2orf71 mutation is associated with atypical Usher syndrome. *J Med Genet*. 2014;51(7):460–469.
8. Neuhaus C, Eisenberger T, Decker C, et al. Next-generation sequencing reveals the mutational landscape of clinically diagnosed Usher syndrome: copy number variations, phenocopies, a predominant target for translational read-through, and PEX26 mutated in Heimler syndrome. *Mol Genet Genomic Med*. 2017;5(5):531–552.
9. Mayor T, Stierhof YD, Tanaka K, Fry AM, Nigg EA. The centrosomal protein C-Nap1 is required for cell cycle-regulated centrosome cohesion. *J Cell Biol*. 2000;151(4):837–846.
10. Prosser SL, Sahota NK, Pelletier L, Morrison CG, Fry AM. Nek5 promotes centrosome integrity in interphase and loss of centrosome cohesion in mitosis. *J Cell Biol*. 2015;209(3):339–348.
11. de Castro-Miró M, Tonda R, Escudero-Ferruz P, et al. Novel candidate genes and a wide spectrum of structural and point mutations responsible for inherited retinal dystrophies revealed by exome sequencing. *PLoS One*. 2016;11(12):e0168966.
12. Kubota D, Gocho K, Kikuchi S, et al. CEP250 mutations associated with mild cone-rod dystrophy and sensorineural hearing loss in a Japanese family. *Ophthalmic Genet*. 2018;39(4):500–507.
13. Fuster-García C, García-García G, Jaijo T, et al. High-throughput sequencing for the molecular diagnosis of Usher syndrome reveals 42 novel mutations and consolidates CEP250 as Usher-like disease causative. *Sci Rep*. 2018;8(1):17113.
14. Huang X-F, Xiang L, Fang X-L, et al. Functional characterization of CEP250 variant identified in nonsyndromic retinitis pigmentosa. *Hum Mutat*. 2019;40(8):1039–1045.
15. Igelman AD, Ku C, da Palma MM, et al. Expanding the clinical phenotype in patients with disease causing variants associated with atypical Usher syndrome. *Ophthalmic Genet*. 2021;42(6):664–673.
16. Gibson F, Walsh J, Mburu P, et al. A type VII myosin encoded by the mouse deafness gene shaker-1. *Nature*. 1995;374(6517):62–64.
17. Alagramam KN, Murcia CL, Kwon HY, Pawlowski KS, Wright CG, Woychik RP. The mouse Ames waltzer hearing-loss mutant is caused by mutation of *Pcdh15*, a novel protocadherin gene. *Nat Genet*. 2001;27(1):99–102.
18. Mburu P, Mustapha M, Varela A, et al. Defects in whirlin, a PDZ domain molecule involved in stereocilia elongation, cause deafness in the whirler mouse and families with DFNB31. *Nat Genet*. 2003;34(4):421–428.
19. Liu X, Bulgakov O V, Darrow KN, et al. Usherin is required for maintenance of retinal photoreceptors and normal development of cochlear hair cells. *Proc Natl Acad Sci USA*. 2007;104(11):4413–4418.

20. Yan D, Liu XZ. Genetics and pathological mechanisms of Usher syndrome. *J Hum Genet*. 2010;55(6):327–335.
21. Skarnes WC, Rosen B, West AP, et al. A conditional knockout resource for the genome-wide study of mouse gene function. *Nature*. 2011;474(7351):337–344.
22. Gerth-Kahlert C, Tiwari A, Hanson JVM, et al. C2orf71 mutations as a frequent cause of autosomal-recessive retinitis pigmentosa: clinical analysis and presentation of 8 novel mutations. *Invest Ophthalmol Vis Sci*. 2017;58(10):3840.
23. Kubota D, Gocho K, Kikuchi S, et al. CEP250 mutations associated with mild cone-rod dystrophy and sensorineural hearing loss in a Japanese family. *Ophthalmic Genet*. 2018;39(4):500–507.
24. Chang B, Hawes NL, Hurd RE, Davisson MT, Nusinowitz S, Heckenlively JR. Retinal degeneration mutants in the mouse. *Vision Res*. 2002;42(4):517–525.
25. Veleri S, Lazar CH, Chang B, Sieving PA, Banin E, Swaroop A. Biology and therapy of inherited retinal degenerative disease: insights from mouse models. *Dis Model Mech*. 2015;8(2):109–129.
26. Williams DS. Usher syndrome: animal models, retinal function of Usher proteins, and prospects for gene therapy. *Vision Res*. 2008;48(3):433–441.
27. Tian G, Lee R, Ropelewski P, Imanishi Y. Impairment of vision in a mouse model of usher syndrome type III. *Invest Ophthalmol Vis Sci*. 2016;57(3):866.
28. Geng R, Melki S, Chen DH-C, et al. The mechanosensory structure of the hair cell requires clarin-1, a protein encoded by Usher syndrome III causative gene. *J Neurosci*. 2012;32(28):9485–9498.
29. Yan W, Long P, Chen T, et al. A natural occurring mouse model with *Adgrv1* mutation of Usher syndrome 2C and characterization of its recombinant inbred strains. *Cell Physiol Biochem*. 2018;47(5):1883–1897.
30. Dona M, Slijkerman R, Lerner K, et al. Usherin defects lead to early-onset retinal dysfunction in zebrafish. *Exp Eye Res*. 2018;173:148–159.
31. Han S, Liu X, Xie S, et al. Knockout of *ush2a* gene in zebrafish causes hearing impairment and late onset rod-cone dystrophy. *Hum Genet*. 2018;137(10):779–794.